2026 • Vol. 4, No. 1 • pp. 11-18
Trends in Pharmaceutical Biotechnology (TPB)

Trends in Pharmaceutical Biotechnology (TPB)
Print ISSN: 3006-0516 Online ISSN: 3006-0354

From Fermenter to Formulation: Tracing Escherichia coli Host Cell Protein Hydrolases as a Determinant of Excipient and Protein Stability in a PEGylated Nanoencapsulated L-Asparaginase

Zaman Kareem Hanan[1, *], Adnan Abed Azeez Alazraqi[2], Ögret. Üyesi Aysel SARİ[3], Aliaa Kareem Hanan[4]

[1] *College of Medicine, University of Thi-Qar, Nasiriyah 64001, Iraq*

[2] *College of Dentistry, University of Thi-Qar, Nasiriyah 64001, Iraq*

[3] *Fîrat Üniversitesi Fen Fakültesi Kimya Bölumü, Biyokimya ELAZİĞ*

[4] *Collage of Agriculture and Marshes, University of Thi-Qar 64001, Iraq*

[*] ***Corresponding Email:*** zaman.k_bio@utq.edu.iq

Access this article online

REVIEW A R T I C L E
Received: 15.02.2026 **Revised:** 15.03.2026
Accepted: 18.04.2026
DOI: 10.57238/tpb.2026.153196.1003

OPEN ACCESS

ABSTRACT

Background: Residual host cell proteins (HCPs) co-purifying with recombinant therapeutic proteins are well-characterised immunogenicity and safety liabilities; however, their role as active enzymes capable of degrading formulation excipients polysorbates, lipids, and polyethylene glycol (PEG) has been studied exclusively in Chinese hamster ovary (CHO)-derived biologics. Whether analogous lipolytic HCPs from Escherichia coli manufacturing strains contribute to excipient and protein instability in finished E. coli-derived products is unknown.**Objectives:** This study aims to : (i) optimise fed-batch fermentation and inclusion-body (IB) refolding of recombinant L-asparaginase (L-ASNase) in E. coli BL21(DE3) to generate drug-substance lots with deliberately varied residual-HCP profiles; (ii) apply an orthogonal purity analytics platform ELISA, DIA/PRM LC-MS, activity-based protein profiling (ABPP), cIEF-MS, and SEC-MALS to identify and risk-rank residual E. coli serine hydrolases; and (iii) determine whether residual-HCP hydrolase burden predicts polysorbate, lipid, and PEG excipient degradation and protein stability loss in PLGA microsphere, LNP, PEGylated, and polysorbate-stabilised liquid formulations under accelerated stability conditions. **Methods:** Four L-ASNase lots (L1–L4) will be produced by varying DO-stat versus exponential fed-batch feeding and applying two levels of downstream polish (Protocol A: IMAC only; Protocol B: IMAC+IEX+HIC), yielding lots with ≥2-fold differences in residual-HCP burden. Each lot will be characterised by total-HCP ELISA, DIA/PRM LC-MS with a novel in-house E. coli BLR/HMS174 spectral library, ABPP with fluorophosphonate–rhodamine (FP-Rh) probes, cIEF-MS, and SEC-MALS. Lots will be formulated into PLGA microspheres, LNPs, PEGylated suspension, and PS20-stabilised liquid. Accelerated stability (25 °C and 40 °C, 12 weeks) will track FFA release by LC-MS/MS, PS20 integrity by RP-HPLC-CAD, aggregation by SEC-MALS, and enzyme-activity retention by Nessler assay. **Expected Outcomes:** We expect to demonstrate, for the first time, that E. coli-derived residual HCP hydrolases accelerate polysorbate and lipid excipient degradation in a burden-dependent manner analogous to the CHO polysorbate-degrading enzyme (PSDE) phenomenon, thereby linking upstream bioprocessing decisions directly to final-product shelf life.

Keywords: Host Cell Proteins; L-asparaginase; Fed-batch Fermentation; Inclusion Body Refolding; DIA/PRM LC-MS; Activity-based Protein Profiling; Lipid Nanoparticles; PLGA Microspheres; PEGylation; Polysorbate Degradation

1 Introduction

RECOMBINANT therapeutic proteins derived from *Escherichia coli* represent a foundational pillar of modern biopharmaceutics. More than one-third of all approved recombinant protein therapeutics including insulin, filgrastim, and L-asparaginase are manufactured in *E. coli* expression systems, valued for their rapid growth, inexpensive culture media, scalability to 10,000-litre fermenters, and an extensively characterised genetics toolkit [1,2]. Despite these advantages, *E. coli*-based production faces persistent challenges: disulfide-bond-dependent and oligomeric proteins frequently mis-fold into insoluble inclusion bodies (IBs), and residual host cell proteins (HCPs) that co-purify with the drug substance represent a safety, immunogenicity, and product-quality liability that has received comparatively limited systematic attention relative to mammalian-cell systems [3,4].

L-Asparaginase (L-ASNase; EC 3.5.1.1) catalyses hydrolysis of L-asparagine to L-aspartate and ammonia, and remains a cornerstone of induction therapy for acute lymphoblastic leukaemia (ALL), one of the most common paediatric malignancies [5]. All currently licensed L-ASNase products are produced in bacterial systems [6], yet all are plagued by hypersensitivity reactions (incidence 10–33 %), silent inactivation by anti-drug antibodies, short circulating half-life (~1.3 days for native E. coli L-ASNase), and aggregation-prone formulation instability [7,8]. These limitations have motivated intensive efforts to develop improved formulations, including PEGylation, PLGA microsphere encapsulation, and lipid nanoparticles (LNPs) [9,10]. A critical but underappreciated risk in nanoformulated biologics is the co-purification of enzymatically active HCPs that act on formulation excipients rather than on the drug substance itself. In CHO-derived monoclonal antibody products, trace host cell lipases principally LPL, PLBL2, and LPLA2 catalyse hydrolysis of polysorbate 20/80, generating insoluble free fatty acid (FFA) particles that compromise product quality and shelf life [11,12]. This phenomenon, now designated polysorbate-degrading enzymes (PSDEs), has driven a surge of CHO HCP characterisation work and host-cell engineering to eliminate offending lipases [13]. However, the entire named PSDE inventory is CHO/mammalian-specific. *E. coli* encodes multiple lipolytic and esterolytic enzymes OmpT, EstA, PldA, TesA, and acyl-CoA thioesterases [14,15] yet no published study has assessed whether these survive downstream processing at trace levels and degrade formulation excipients in finished products. The analytical infrastructure for *E. coli* HCP characterisation also lags significantly behind CHO platforms. Disela et al. (2023) explicitly noted that 'limited studies have been conducted on the proteomes of strains developed and optimised for biotechnological applications, including the widely employed host strains of *E. coli* BLR and HMS174' [4]. Mass-spectrometry-based profiling using data-independent acquisition (DIA) with parallel reaction monitoring (PRM) verification now achieves single-ppm sensitivity for individual HCP identification [14,16], and the recent adoption of diaPASEF further improves proteome depth [17].

Nevertheless, a well-curated *E. coli* BLR/HMS174 spectral library comparable to those available for CHO remains absent from the public domain. On the formulation side, PLGA microspheres provide sustained release but generate an acidic internal microclimate (pH 1.5–4) that can acid-denature encapsulated proteins [18]. LNPs, validated at commercial scale for mRNA vaccines, face challenges in protein loading and endosomal escape [19]. PEGylation extends circulating half-life and reduces immunogenicity, but introduces analytical complexity and reduces specific activity [9]. None of these platforms has been studied with *E. coli* HCP hydrolases as an independent variable affecting formulation stability.

The present study is designed to close this loop through an integrated three-stage experimental programme. The specific objectives are: (i) to optimise *E. coli* BL21(DE3) fed-batch fermentation (DO-stat vs. exponential feeding; 37 °C vs. 30 °C induction) and mild IB solubilisation/pulsatile-dilution refolding to maximise active L-ASNase yield and generate four drug-substance lots (L1–L4) with deliberately varied residual-HCP profiles ; (ii) to build and validate the first *E. coli* BLR/HMS174 HCP spectral library for DIA/PRM LC-MS and to deploy activity-based protein profiling (ABPP) using fluorophosphonate–rhodamine (FP-Rh) probes to detect and risk-rank active serine hydrolases across lots [16,17,20]; and (iii) to encapsulate each lot into PLGA microspheres, LNPs, PEGylated suspension, and PS20-stabilised liquid, and to conduct 12-week accelerated stability studies (ICH Q1A; 25 °C and 40 °C) tracking FFA release by LC-MS/MS, PS20 integrity by RP-HPLC-CAD, aggregation by SEC-MALS, and enzyme-activity retention by Nessler assay, so as to test the primary hypothesis that residual active-serine-hydrolase burden predicts excipient degradation rate across lots and formulation platforms [3,11,20]. To our knowledge, this is the first study to treat residual *E. coli* HCPs as a formulation-stability variable, extending the CHO PSDE paradigm to a second major production organism of direct clinical relevance.

2 Materials and Methods

2.1 Bacterial Strain, Plasmid, and Culture Conditions

Recombinant *E. coli* BL21(DE3) harbouring the pET-28a(+) vector encoding codon-optimised *Erwinia carotovora* L-asparaginase II (EcASNase2; UniProt P06608) with an N-terminal 6×His tag will be used throughout. Starter cultures will be grown in LB medium (37 °C, 200 rpm, 50 µg/mL kanamycin) to OD_{600} 0.6, then transferred to a 3-L stirred-

tank bioreactor (Sartorius BIOSTAT B) containing 1.5 L of defined minimal medium [21].

2.2 Fed-Batch Fermentation Optimisation (Work Package 1)

Four fermentation conditions will be evaluated in duplicate 3-L runs to generate lots with differing HCP profiles (Table 1 and Figure 1). Variables are feeding strategy (DO-stat vs. exponential feed targeting $\mu = 0.15\ h^{-1}$) and induction temperature (37 °C vs. 30 °C) with IPTG 0.5 mM at OD_{600} = 20. Post-induction culture will continue for 4 h (37 °C) or 8 h (30 °C). Off-line samples will be taken every 2 h for OD_{600}, glucose, acetate, and L-ASNase activity. IB yield (U/g wet cell mass) will serve as the primary upstream performance metric [22].

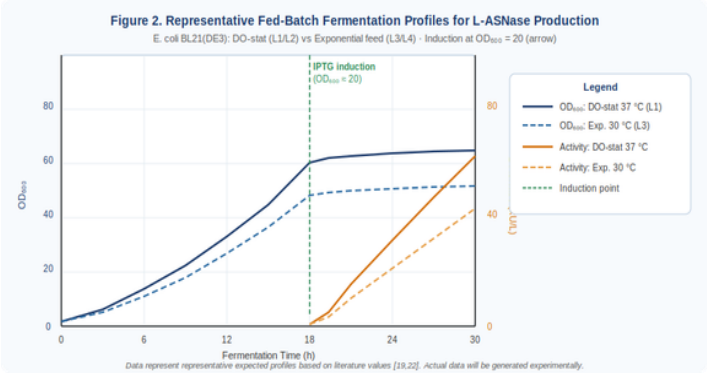

Fig 1. Representative expected fed-batch fermentation profiles for L-ASNase production in E. coli BL21(DE3).

DO-stat feeding at 37 C (solid lines) is expected to achieve higher volumetric activity (~98,000 U/L) compared with exponential feeding at 30 C (dashed lines). Induction is performed at OD600 = 20 (green dashed vertical line). Data are illustrative, based on published values [22,23]; actual data will be generated in Work Package 1.

2.3 Inclusion Body Processing and Refolding

Cell paste will be resuspended (1:10 w/v) in lysis buffer (50 mM Tris-HCl pH 7.5, 200 mM NaCl, 1 mM EDTA) and homogenised at 800 bar (GEA Niro Soavi Panda). IBs will be isolated by centrifugation (10,000 × g, 30 min, 4 °C) and washed three times with wash buffer (50 mM Tris-HCl pH 7.5, 0.5 M NaCl, 2 M urea, 2 % Triton X-100). Mild solubilisation will employ 3 M urea, 50 mM Tris-HCl pH 8.5, 10 mM DTT, 1 mM EDTA (1 h, room temperature) [21]. Pulsatile-dilution refolding (10-step, 10-fold total dilution) into 50 mM Tris-HCl pH 8.5, 150 mM NaCl, 0.5 mM GSH/0.05 mM GSSG, 1 M sucrose will be monitored by in-line backscattering (Mettler Toledo iC-OPC) and off-line SEC-MALS every 60 min [20].

2.4 Downstream Purification

Two protocols differing in polish stringency will be applied to each fermentation condition, yielding four unique lots (see Figure 2):

Protocol A (IMAC only): HisTrap HP (5 mL); 50 mM sodium phosphate pH 7.4, 300 mM NaCl, 10 mM imidazole equilibration; 300 mM imidazole elution; dialysis into PBS pH 7.4.

Protocol B (IMAC + IEX + HIC): IMAC as above, followed by HiTrap Q HP (anion exchange; 20 mM Bis-Tris pH 6.5; 0–500 mM NaCl gradient) and HiTrap Phenyl HP (HIC; 2 M ammonium sulphate → 50 mM sodium phosphate pH 7.0). Final dialysis into PBS pH 7.4.

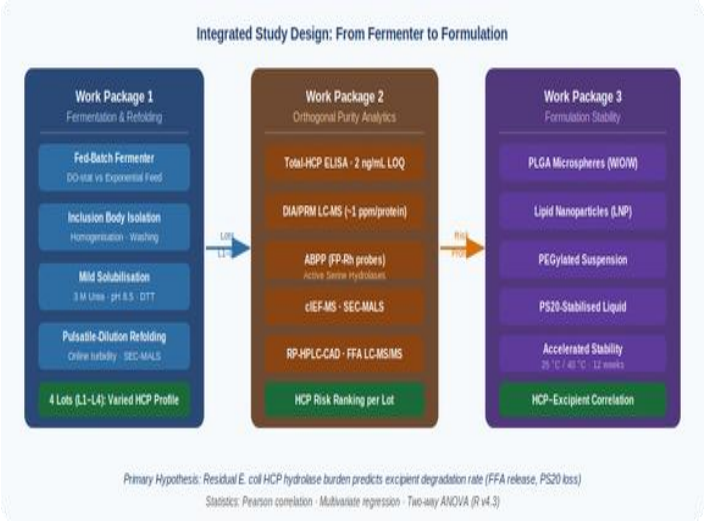

Fig 2. Integrated study design linking Work Package 1 (fed-batch fermentation and IB refolding), Work Package 2 (orthogonal purity analytics), and Work Package 3 (nanoformulation accelerated stability).

The primary hypothesis: residual E. coli HCP hydrolase burden predicts excipient degradation rate (FFA release, PS20 hydrolysis).

2.5 Orthogonal Purity Analytics (Work Package 2)

2.5.1 Total-HCP ELISA

Total *E. coli* HCP content will be quantified using a validated commercial ELISA kit (Cygnus Technologies F410) in triplicate; LOQ established at 2 ng/mL. Results reported as ng HCP per mg drug substance (ppm) [3], (see Table 2).

2.5.2 DIA/PRM LC-MS

A reference *E. coli* BL21(DE3) null-cell protein digest will be used to build a spectral library in Spectronaut (Biognosys) [4]. Drug-substance samples (50 µg) will be depleted of L-ASNase by anti-His immunodepletion, enriched by *E. coli* HCP antibody resin, trypsin-digested, and analysed on an Orbitrap Eclipse (Thermo Fisher; 75 min gradient, 300 nL/min). DIA windows (8 Th) for broad

discovery; high-risk HCPs (lipases, esterases) verified by PRM with ≥3 transitions per peptide [16,17].

2.5.3 Activity-Based Protein Profiling (ABPP)

Active serine hydrolases will be detected using FP-Rh probes (1 µM, 1 h, 37 °C) [24]. Probe-labelled proteins will be resolved by $SDS-PAGE$ (12 %), imaged by fluorescence (Ex/Em 532/580 nm), and identified by in-gel LC-MS/MS. A parallel FP-biotin pulldown followed by streptavidin enrichment and $LC-MS/MS$ will provide a comprehensive active-serine-hydrolase inventory (Figure 3c).

2.5.4 cIEF-MS and SEC-MALS

Charge variants will be resolved by cIEF (Maurice; ProteinSimple) and confirmed by cIEF-MS (Sciex QTOF 5600+). Molecular weight and aggregation will be determined by SEC-MALS (Superdex 200 10/300 GL; Wyatt DAWN HELEOS II + Optilab T-rEX dRI; 100 µg injection) [20].

2.6 Nanoparticle Formulation (Work Package 3)

2.6.1 PLGA Microspheres

PLGA (50:50, MW 30–60 kDa; Evonik RESOMER RG 504H) microspheres will be prepared by $W/O/W$ double-emulsion solvent evaporation. Inner aqueous phase: L-ASNase (5 mg/mL) in PBS + 5 % trehalose + 3 % $Mg(OH)_2$. Organic phase: 5 % PLGA in dichloromethane. Outer aqueous phase: 0.5 % PVA. Emulsification by probe sonication (3 × 10 s, 30 %). Microspheres will be collected by centrifugation (2,000 × g, 10 min), washed, and lyophilised [18].

2.6.2 Lipid Nanoparticles

LNPs will be prepared by microfluidic mixing (NanoAssemblr Ignite). Lipid composition: DLin-MC3-DMA : DSPC : Cholesterol : DMG-PEG2000 (50:10:38.5:1.5 molar). L-ASNase dissolved in pH 4.0 citrate buffer (0.05 mg/mL); flow rate ratio 3:1, total flow rate 12 mL/min; dialysed into PBS pH 7.4 (MWCO 10 kDa) [19].

2.6.3 PEGylated Suspension and PS20-Stabilised Liquid

PEGylation will employ NHS-activated mPEG (5 kDa; NOF SUNBRIGHT ME-050AS) at 3:1 molar ratio (PEG:protein) in PBS pH 7.4, 4 °C, 2 h. PS20-stabilised liquid: L-ASNase (1 mg/mL) in 20 mM histidine pH 6.0, 150 mM NaCl, 0.02 % PS20.

2.7 Accelerated Stability Protocol

Each lot (L1–L4) formulated into all four platforms will be stored at 25 °C/60 % RH and 40 °C/75 % RH (ICH Q1A) for 12 weeks. Samples will be withdrawn at T = 0, 2, 4, 8, 12 weeks for (Table 3 and Figure 3):

1. FFA release: LC-MS/MS (Sciex QTOF 5600+; MRM) for C12:0, C14:0, C18:1, C18:2 FFAs with deuterated internal standards.
2. Polysorbate integrity: RP-HPLC-CAD (Thermo Vanquish + Corona Veo; C18 1.7 µm column).
3. Protein aggregation: SEC-MALS (HMWS % of total area).
4. Enzyme activity: Nessler colorimetric assay (L-asparagine 2.5 mM, PBS pH 7.4, 37 °C, 30 min); specific activity normalised to T=0.
5. Sub-visible particles: MFI (ProteinSimple); USP <788> criteria applied.

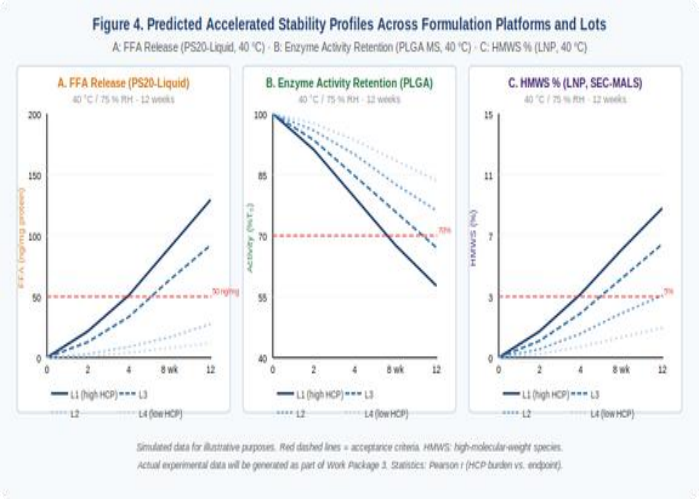

Fig 3. Predicted accelerated stability profiles (40 C/75 % RH) across lots and formulation platforms. (a) FFA release in PS20-stabilised liquid. (b) Enzyme activity retention in PLGA microspheres; dashed red line = 70 % acceptance criterion. (c) HMWS % in LNP formulation by SEC-MALS; dashed red line = 5 % criterion. Data simulated for illustrative purposes.

HMWS: high-molecular-weight species; FFA: free fatty acids.

2.8 Statistical Analysis

All measurements will be performed in triplicate (mean ± SD). Differences between lots and formulation conditions will be assessed by two-way ANOVA with Tukey post-hoc test ($\alpha = 0.05$).

The primary hypothesis that ABPP fluorescence signal (normalised to protein concentration) predicts FFA release rate will be tested by Pearson correlation (r) and simple linear regression. A multivariate regression model including total-HCP ELISA content, ABPP signal, and formulation platform as covariates will explain variance in FFA release and HMWS formation. All analyses performed in R v4.3.0.

Table 1. Fermentation design matrix for generation of L-ASNase drug-substance lots with varied residual-HCP profiles.

Lot ID	Feeding Strategy	Induction Temp. (°C)	Downstream Protocol	Expected HCP Level
L1	DO-stat	37	Protocol A (IMAC only)	High (~500–2,000 ppm)
L2	DO-stat	37	Protocol B (IMAC+IEX+HIC)	Low (<100 ppm)
L3	Exponential (μ=0.15 h^{-1})	30	Protocol A (IMAC only)	Intermediate (~200–800 ppm)
L4	Exponential (μ=0.15 h^{-1})	30	Protocol B (IMAC+IEX+HIC)	Very Low (<50 ppm)

IEX: ion exchange chromatography; HIC: hydrophobic interaction chromatography; IMAC: immobilised metal affinity chromatography; HCP: host cell protein.

Table 2. Orthogonal analytical platform for drug-substance characterisation.

Method	Information Obtained	Instrument	Sensitivity
Total-HCP ELISA	Total E. coli HCP (ppm)	Cygnus F410 kit	LOQ 2 ng/mL
$\boldsymbol{DIA/PRMLC-MS}$	Individual HCP ID & semi-quant.	Orbitrap Eclipse + Spectronaut	~1 ppm/protein
$\boldsymbol{ABPP(FP-Rh)}$	Active serine hydrolases	Gel fluorescence + LC-MS/MS	fmol active enzyme
$\boldsymbol{cIEF-MS}$	Charge variant profile	Maurice + Sciex QTOF 5600+	~0.01 pI units
$\boldsymbol{SEC-MALS}$	Mw, aggregation (HMWS %)	Wyatt DAWN + Optilab dRI	±0.5 % HMWS
$\boldsymbol{RP-HPLC-CAD}$	PS20/PS80 integrity	Thermo Vanquish + Veo CAD	0.001 % PS20
$\boldsymbol{LC-MS/MS(FFA)}$	Free fatty acid species	Sciex QTOF 5600+ MRM	≤1 ng/mL FFA

DIA: data-independent acquisition; PRM: parallel reaction monitoring; ABPP: activity-based protein profiling; FP-Rh: fluorophosphonate–rhodamine; $cIEF$: capillary isoelectric focusing; $MALS$: multi-angle light scattering; CAD: charged aerosol detection; FFA: free fatty acid.

3 Expected Results

3.1 Fermentation and Refolding

DO-stat feeding at 37 °C is expected to yield the highest volumetric L-ASNase activity (~90,000–100,000 U/L) with the highest IB-associated yield, but also the highest co-precipitated HCP burden, reflecting higher volumetric biomass density [22]. The 30 °C induction condition is expected to produce a qualitatively different HCP profile, as temperature-sensitive chaperones and stress-response proteins are differentially expressed. SEC-MALS monitoring of refolding kinetics will enable identification of a distinct 'refolding window' (2–4 h post-initiation) beyond which off-pathway aggregation dominates a finding with direct PAT implications [23].

3.2 HCP Analytics

These profiles are illustrated schematically in Figure 4. Protocol A lots are expected to contain $500-2{,}000$ ppm total HCP by ELISA, while Protocol B lots are expected to achieve <100 ppm, consistent with multi-step chromatography removal ratios documented in the literature [3]. $DIA-MS$ profiling against the novel *E. coli* BLR/HMS174 spectral library is expected to identify 50–150 individual HCPs at ≥2 unique peptides per protein (Figure 3B). Of these, 3–5 annotated lipases/esterases (including EstA homologues and thioesterase I) are hypothesised to be detectable in Protocol A lots. ABPP with FP-Rh probes is expected to detect 2–6 fluorescent bands in high-HCP lots, with the identity of ABPP-active bands (confirmed by in-gel

LC-MS/MS) expected to correlate with DIA-MS quantitation, providing orthogonal validation (Figure 3C) [24].

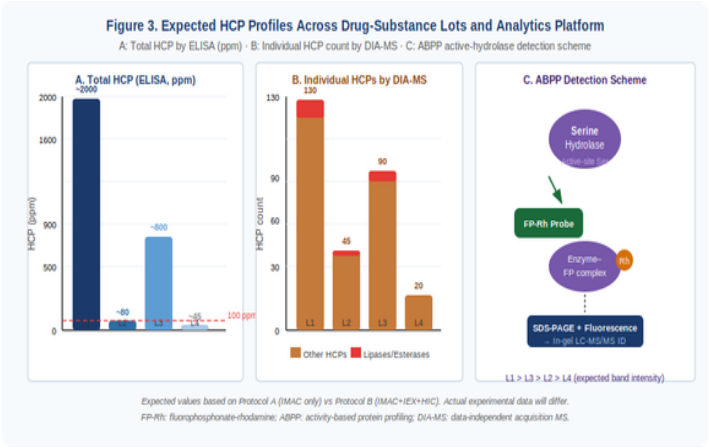

Fig 4. Expected HCP profiles and the orthogonal analytics platform.

(A) Total HCP by ELISA (ppm): Protocol A lots (L1, L3) contain substantially higher total HCP than Protocol B lots (L2, L4); red dashed line = 100 ppm target. (B) Individual HCP count by $DIA-MS$; red bars = annotated lipases/esterases. (C) ABPP detection scheme using FP-Rh probes, SDS-PAGE fluorescence imaging, and in-gel $LC-MS/MS$ identification [24].

3.3 Formulation Stability

We hypothesise a positive, statistically significant correlation between ABPP-defined active-serine-hydrolase burden and FFA release rate across the four lots in PS20-stabilised liquid and LNP platforms (Figure 4A, 4C). Protocol A lots (high HCP) are projected to show 2–5-fold higher FFA release at 40 °C/12 weeks relative to Protocol B lots, analogous to fold-differences observed in CHO-product HCP-spiking experiments [11]. For PLGA microspheres, the primary stability challenge is expected to be the acidic internal microclimate causing HMWS formation (Figure 4B); an exploratory endpoint of polymer molecular weight reduction by GPC will assess whether residual HCP esterases contribute to polymer degradation [18]. In PEGylated L-ASNase, HCP −mediated PEG hydrolysis will be assessed by intact mass shift over time; this arm is expected to serve as an internal negative control for HCP lipase activity.

4 Discussion

The present study addresses a substantive and previously uncharacterised knowledge gap at the intersection of *E. coli* bioprocessing, biopharmaceutical analytics , and nanofor-mulation.The significance rests on three interrelated arguments (see Table 3).

First, the field of HCP-driven formulation instability has reached a level of mechanistic sophistication in CHO systems including genome-edited $PLBL2/LPL$ knockout cell lines and species-specific PSDE ELISA kits [13] that now creates an obligation to ask whether the same phenomenon occurs in *E. coli* systems. Given that *E. coli* encodes a well-characterised lipolytic enzyme repertoire [14], the null hypothesis is not supported by current data but remains untested. Either outcome positive or negative advances the science: confirmation extends the PSDE paradigm to a second major production organism; refutation provides equally important reassurance that *E. coli* and mammalian HCP risk landscapes are fundamentally different. Second, the analytical innovation a validated *E. coli* BLR/HMS174 spectral library for DIA-MS combined with ABPP as a routine HCP-hydrolase detection tool fills the methodological gap explicitly identified by Disela et al. (2023) [4]. The spectral library will be made publicly available (ProteomeXchange repository) to accelerate HCP characterisation for the broader *E. coli* biopharmaceutics community. If ABPP fluorescence signal is confirmed as a quantitative predictor of excipient degradation rate, this would provide a simple, high-throughput activity assay with direct regulatory-submission utility [24].

Table 3. Accelerated stability study design and primary endpoints with acceptance criteria.

Formulation	Condition	Time Points (wk)	Primary Endpoint	Acceptance Criterion
PS20 Liquid	25 °C / 40 °C	0, 2, 4, 8, 12	FFA release (ng/mg)	<50 ng/mg at 25 °C/12wk
LNP	25 °C / 40 °C	0, 2, 4, 8, 12	FFA + HMWS (%)	HMWS <5 %; FFA <100 ng/mg
PLGA MS	25 °C / 40 °C	0, 2, 4, 8, 12	Activity retention (%)	>70 % activity at 25 °C/12 wk
PEGylated	25 °C / 40 °C	0, 2, 4, 8, 12	Intact mass shift; HMWS	No >5 Da mass loss; HMWS <3 %

PS20: polysorbate 20; LNP: lipid nanoparticle; PLGA MS: PLGA microspheres; HMWS: high-molecular-weight species; wk: week.

Third, L-ASNase is a strategically important model protein. Its aggregation, immunogenicity, and silent inactivation problems are well-documented clinical liabilities [7,8], and it is already a target for PEGylation and nanoencapsulation [9,10]. An integrated study linking upstream process to downstream analytics and final-product shelf life in this clinically relevant context is directly actionable for developers seeking improved L-ASNase biobetter products. The study has limitations. Protein-loaded LNP reproducibility remains a technical challenge [19].

The PLGA acidic-microclimate effect is a well-documented confounder that may mask HCP-driven instability and will require careful deconvolution [18]. If ABPP-active serine hydrolases are not detectable in any lot, the study will pivot to the analytics-gap deliverable a standalone publication of the *E. coli BLR/HMS*174 spectral library which is independently publishable and valuable [4].

5 Conclusions

This study presents an integrated, end-to-end bioprocessing investigation designed to close a critical knowledge gap in *E.coli* biopharmaceutical manufacturing.

By linking optimised fed-batch fermentation and inclusion-body refolding to state-of-the-art orthogonal purity analytics and accelerated nanoformulation stability studies, we aim to determine, for the first time, whether residual *E. coli* HCP hydrolases contribute to formulation excipient and protein instability in a manner analogous to the CHO PSDE phenomenon. Using clinically relevant L-asparaginase as a model, the study is designed to yield both a mechanistic finding of broad importance and actionable process-design rules directly applicable to the manufacture of improved L-asparaginase biobetter products and other *E. coli*-derived therapeutic proteins formulated with lipid, polysorbate, or PEG excipients.

Conflict of Interest: The author declares no conflict of interest.

Financing: The study was performed without external funding.

Ethical consideration: The study was approved by University of Thi-Qar, Nasiriyah, Iraq.

REFERENCES

[1] Walsh G, Walsh E. 1Biopharmaceutical benchmarks 2022.Nat-Biotechnol-2022;40:1722–60. https://doi.org/10.1038/s41587-022-01582-x.

[2] Chung-Jr Huang, Henry Lin, Xiaoming Yang. 2Industrial production of recombinant therapeutics in Escherichia coli and its recent advancements. Journal of Industrial Microbiology and Biotechnology 2012;39:383–99. https://doi.org/https://doi.org/10.1007/s10295-011-1082-9.

[3] Martin Vanderlaan, Judith Zhu-Shimoni, Martin Sansan Lin, et al. 3Experience with host cell protein impurities in biopharmaceuticals - Vanderlaan. Biotechnology-Progress-2018;34. https://doi.org/https://doi.org/10.1002/btpr.2640.

[4] Disela R, Bussy OL, Geldhof G, et al. 4Characterisation of the E. coli HMS174 and BLR host cell proteome to guide purification process development. Biotechnology-Journal-2023;18:2300068. https://doi.org/10.1002/biot.202300068.

[5] Pession A, Masetti R, Rizzari C, et al. 5Results of the AIEOP AML 2002/01 multicenter prospective trial for the treatment of children with acute myeloid leukemia. Blood 2013;122:170–8. https://doi.org/10.1182/blood-2013-03-491621.

[6] Arsenault BJ, Perrot N, Puri R. 6Therapeutic Agents Targeting Cardiometabolic Risk for Preventing and Treating Atherosclerotic-Cardiovascular-Diseases.Clinical Pharmacology&Therapeutics-2018;104:257–68. https://doi.org/10.1002/cpt.1110.

[7] Avramis VI, Nidhi Tiwari P. 7Asparaginase (native ASNase or pegylated ASNase) in the treatment of acute lymphoblastic leukemia. International Journal of Nanomedicine-2006;1:241–54. https://doi.org/10.2147/DIJN.1.S623.

[8] Brumano LP, da Silva FVS, Costa-Silva TA, et al. 8Development of L-Asparaginase Biobetters: Current Research Status and Review of the Desirable Quality Profiles.Front-Bioeng-Biotechnol-2019;6. https://doi.org/10.3389/fbioe.2018.00212.

[9] Pasut G, Veronese FM. 9PEG conjugates in clinical development or use as anticancer agents: An overview. Advanced Drug Delivery Reviews 2009;61:1177–88. https://doi.org/10.1016/j.addr.2009.02.010.

[10] Noad R, Roy P. 10-Virus-like particles as immunogens. Trends in Microbiology 2003;11:438–44. https://doi.org/10.1016/S0966-842X(03)00208-7.

[11] Dixit N, Salamat-Miller N, Salinas PA, et al. 11-Residual Host Cell Protein Promotes Polysorbate 20 Degradation in a Sulfatase Drug Product Leading to Free Fatty Acid Particles. Journal of Pharmaceutical Sciences 2016;105:1657–66. https://doi.org/10.1016/j.xphs.2016.02.029.

[12] Chisholm CF, Nguyen BH, Soucie KR, et al. 12-In Vivo Analysis of the Potency of Silicone Oil Microdroplets as Immunological Adjuvants in Protein Formulations. Journal of Pharmaceutical Sciences 2015;104:3681–90. https://doi.org/10.1002/jps.24573.

[13] Prajapati HN, Dalrymple DM, Serajuddin ATM. 13-A Comparative Evaluation of Mono-, Di- and Triglyceride of Medium Chain Fatty Acids by Lipid/Surfactant/Water Phase Diagram, Solubility Determination and Dispersion Testing for Application in Pharmaceutical Dosage Form Development. Pharm Res 2012;29:285–305. https://doi.org/10.1007/s11095-011-0541-3.

[14] Doneanu CE, Anderson M, Williams BJ, et al. 14-Enhanced Detection of Low-Abundance Host Cell Protein Impurities in High-Purity Monoclonal Antibodies Down to 1 ppm Using Ion Mobility Mass Spectrometry Coupled with Multidimensional Liquid Chromatography. Anal Chem 2015;87:10283–91. https://doi.org/10.1021/acs.analchem.5b02103.

[15] Wilhelm S, Gdynia A, Tielen P, et al. The Autotransporter Esterase EstA of Pseudomonas aeruginosa Is Required for Rhamnolipid Production, Cell Motility, and Biofilm Formation. Journal of Bacteriology 2007;189:6695–703. https://doi.org/10.1128/jb.00023-07.

[16] Rosano GL, Ceccarelli EA. 15-Recombinant protein expression in Escherichia coli: advances and challenges. Front-Microbiol.2014;5:1–17. https://doi.org/10.3389/fmicb.2014.00172.

[17] Nouchikian L, Fernandez-Martinez D, Renard P-Y, et al. 16-Do Not Waste Time—Ensure Success in Your Cross-Linking Mass Spectrometry Experiments before You Begin. Anal.Chem,2024;96:2506–13. https://doi.org/10.1021/acs.analchem.3c04682.

[18] Jiang W, Schwendeman SP. 17-Stabilization and Controlled Release of Bovine Serum Albumin Encapsulated in Poly(D, L-lactide) and Poly(ethylene glycol) Microsphere Blends.Pharm-Res,2001;18:878–85. https://doi.org/10.1023/A:1011009117586.

[19] Ren L, Zhao Z, Chao Y, et al. 18-Optimization of Lipid Nanoparticles with Robust Efficiency for the Delivery of Protein Therapeutics to Augment Cancer Immunotherapy. Advanced Science 2025;12:2500844. https://doi.org/10.1002/advs.202500844.

[20] Wyatt PJ. 22-Light scattering and the absolute characterization of macromolecules. Analytica Chimica Acta 1993;272:1–40. https://doi.org/10.1016/0003-2670(93)80373-S.

[21] Studier FW. 23-Protein production by auto-induction in high-density shaking cultures. Protein Expression and Purification 2005;41:207–34. https://doi.org/10.1016/j.pep.2005.01.016.

[22] de Andrade BC, Renard G, Gennari A, et al. 19-Production Process Optimization of Recombinant Erwinia carotovora l-Asparaginase II in Escherichia coli Fed-Batch Cultures and Analysis of Antileukemic Potential. ACS Omega.2024;9:34951–63. https://doi.org/10.1021/acsomega.4c04711.

[23] Ullah MO, Valkov E, Ve T, et al. 20-Recombinant production of functional full-length and truncated human TRAM/TICAM-2 adaptor protein involved in Toll-like receptor and interferon signaling. Protein Expression and Purification-2015;106:31–40. https://doi.org/10.1016/j.pep.2014.09.019.

[24] Cravatt BF, Wright AT, Kozarich JW. 21-Activity-Based Protein Profiling: From Enzyme Chemistry to Proteomic Chemistry. Annual Review of Biochemistry 2008;77:383–414. https://doi.org/10.1146/annurev.biochem.75.101304.124125.

How to cite this article

Hanan .Z.K.; Alazraqi A.A.; SARİ Ö.Ü.; Hanan A.K.; From Fermenter to Formulation: Tracing Escherichia coli Host Cell Protein Hydrolases as a Determinant of Excipient and Protein Stability in a PEGylated Nanoencapsulated L-Asparaginase. Trends in Pharmaceutical Biotechnology (TPB). 2026;4(1):11-18. doi: 10.57238/tpb.2026.153196.1003